

MagicComp: Training-free Dual-Phase Refinement for Compositional Video Generation

Hongyu Zhang^{1*} Yufan Deng^{1*} Shenghai Yuan¹ Peng Jin¹
 Zesen Cheng¹ Yian Zhao¹ Chang Liu³ Jie Chen^{1,2}✉

¹School of Electronic and Computer Engineering, Peking University, Shenzhen, China

²Peng Cheng Laboratory, Shenzhen, China.

³Tsinghua University, Beijing, China

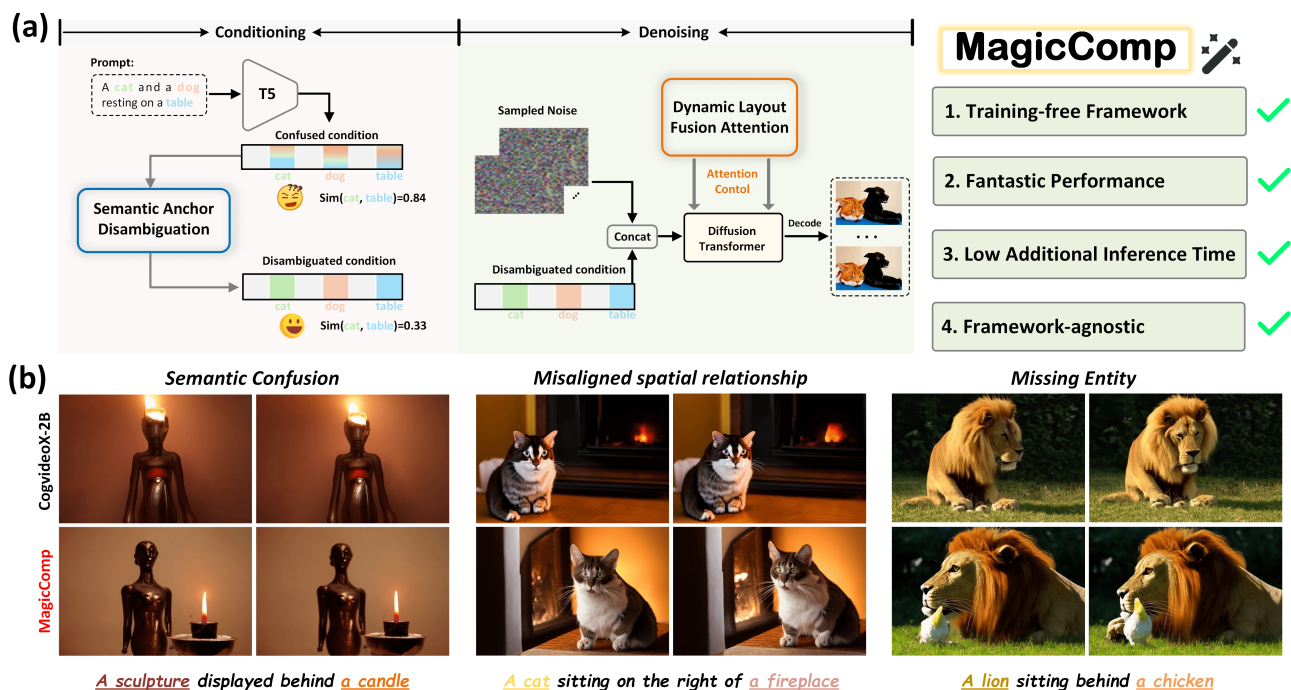


Figure 1. **Overall pipeline for MagicComp.** (a) Our MagicComp comprises two core modules: Semantic Anchor Disambiguation (SAD) for resolving inter-subject ambiguity during conditioning, and Dynamic Layout Fusion Attention (DLFA) for spatial-attribute binding via fused layout masks in denoising. (b) MagicComp is a training-free framework, which effectively address the challenges (e.g., semantic confusion, misaligned spatial relationship, missing entities) in compositional video generation with minimal additional inference overhead.

Abstract

Text-to-video (T2V) generation has made significant strides with diffusion models. However, existing methods still struggle with accurately binding attributes, determining spatial relationships, and capturing complex action interactions between multiple subjects. To address these limitations, we propose **MagicComp**, a training-free method that enhances compositional T2V generation through dual-phase refinement. Specifically, (1) During the Conditioning Stage: We introduce the Semantic Anchor Disambiguation

to reinforces subject-specific semantics and resolve inter-subject ambiguity by progressively injecting the directional vectors of semantic anchors into original text embedding; (2) During the Denoising Stage: We propose Dynamic Layout Fusion Attention, which integrates grounding priors and model-adaptive spatial perception to flexibly bind subjects to their spatiotemporal regions through masked attention modulation. Furthermore, MagicComp is a model-agnostic and versatile approach, which can be seamlessly integrated into existing T2V architectures. Extensive experiments on T2V-CompBench and VBench demonstrate that MagicComp outperforms state-of-the-art methods, highlight-

✉ Corresponding author. * Equal contribution.

ing its potential for applications such as complex prompt-based and trajectory-controllable video generation. Project page: <https://hong-yu-zhang.github.io/MagicComp-Page/>.

1. Introduction

Recent text-to-video (T2V) generation has achieved significant breakthroughs, driven by the scaling of data and model sizes [10, 16, 42, 49, 51, 52] as well as the development of novel network architectures [1, 3–5, 25, 32]. These advancements are propelling the field toward a new era of high-quality visual content synthesis [15, 22, 27, 48, 50]. However, existing models consistently struggle to process prompts involving compositional semantics, especially those with multiple subjects, intricate spatial configurations, and dynamic interactions. These limitations often lead to issues such as semantic leakage, misaligned spatial relationships, and subject missing, making compositional T2V generation a persistently challenging task [39].

To address these challenges, existing methods primarily adopt two strategies: (1) Layout-based approaches, which leverage object-grounding layouts to achieve attribute and motion binding for individual subjects through masked attention mechanisms [12, 26, 40, 43]. (2) Inference-enhanced approaches, which employ multi-round evaluations [19, 24] based on large language models (LLMs) [34] and multi-modal large language models (MLLMs) [33], or conduct test-time optimization [47] to iteratively refine the generation process and enhance compositional quality. However, these methods still exhibit significant limitations: (1) Coarse grounding conditions, such as blobs and 2D bounding boxes, fail to capture fine-grained shape variations, leading to unnatural and inconsistent subject appearances. Additionally, existing layout-based approaches require either large-scale fine-tuning or LoRA tuning [17], both of which impose computational and training overhead. (2) While test-time optimization and multi-round evaluation improve quality, they considerably increase substantial inference burdens. Therefore, developing a training-free compositional video generation framework that achieves high-quality results without significantly increasing inference time remains a critical yet underexplored challenge.

The primary challenge in compositional T2V lies in addressing two interrelated objectives: (1) preventing semantic ambiguity and leakage among multiple subjects and (2) ensuring precise attribute–location binding for each subject across temporal sequences. Notably, achieving both objectives simultaneously is challenging, especially when the model is frozen. A natural approach, therefore, is to decompose these objectives into distinct phases during sampling, enabling progressive refinement at each stage.

Guided by the preceding analysis and insights, we pro-

pose MagicComp, a training-free framework that incrementally resolves inter-subject semantic disambiguation and achieves spatio-temporal binding between subjects and their textual prompts through sequential refinement. During the conditioning phase, text encoders might produce semantically ambiguous embeddings, where distinct subjects (e.g., "dog" vs. "table") exhibit unexpectedly high similarity due to cross-token interference. To address this, we introduce the *Semantic Anchor Disambiguation (SAD)*, which generates the subject anchor embeddings through independently encoding each subject, then computes directional vectors between these anchors and adaptively integrates them into the original text embeddings. The strength of this integration is dynamically modulated by semantic confusion scales and denoising timesteps, ensuring a balance between semantic disambiguation and contextual coherence. During the denoising stage, we present the *Dynamic Layout Fusion Attention (DLFA)* to establish precise spatio-temporal binding between each subject and its associated attributes and locations. Unlike previous approaches [40, 43] that rigidly constrain attention with predefined masks, DLFA first estimates coarse subject layouts via LLM-generated priors, then dynamically refines them through model-adaptive perception of the correlation between subject-specific text embeddings and video token embeddings, enabling fine-grained control over each subject’s shape and details. By integrating the SAD with DLFA, we introduce MagicComp, a training-free and model-agnostic framework that seamlessly enhances mainstream architectures (e.g., DiT-based and UNet-based approaches) and achieves substantial improvements in compositional T2V tasks.

We incorporate MagicComp into both CogVideoX [48] and VideoCrafter2 [8], and evaluate its performance on T2V-CompBench [39] and VBench [20]. Quantitative comparisons across these benchmarks demonstrate that our method achieves superior performance. Beyond standard metrics, we highlight its applicability in complex prompt-based and trajectory-controllable video generation scenarios, emphasizing its versatility and practical potential. Our contributions are summarized as follows:

- We propose MagicComp, a model-agnostic approach for compositional text-to-video generation that avoids additional training or parameter updates. This design significantly reduces overhead and inference time, making compositional video synthesis more efficient and practical.
- We introduce two key modules: (i) Semantic Anchor Disambiguation (SAD), which enhances subject-specific semantics and eliminates inter-subject ambiguity through adaptive integration of semantic anchors’ directional guidance into text embeddings; and (ii) Dynamic Layout Fusion Attention (DLFA), which ensures spatio-temporal subject consistency by combining LLM prior layouts with model-adaptive perception layouts to achieve more flexi-

ble attention modulations.

- Comprehensive results on T2V-CompBench and VBench demonstrate MagicComp’s superior performance compared to state-of-the-art compositional methods.

2. Related Work

Text-to-video generation. Early methods [2, 6, 8, 21, 41], such as MagicTime [51, 52] and AnimateDiff [14], integrating temporal modules into the 2D U-Net architecture [38], thereby seamlessly extending image generation models to video generation models. More recent works, including OpenSora Plan [27], CogVideoX [48], LTX-Video [15], and HunyuanVideo [23], incorporate a 3D full-attention mechanism, recognized for its superior scalability [32]. This advantage significantly enhances model’s ability to capture dynamics in video data, driving rapid progress in T2V [7, 9, 11, 25, 46, 50, 53]. However, these methods still face challenges in accurately preserving attribute consistency, modeling spatial relationships, and capturing complex interactions among multiple subjects, further research are required to address these limitations.

Compositional video generation. Compositional video generation remains a challenging task, particularly in managing multiple objects and their interactions across spatial and temporal dimensions. While compositional image generation has seen significant advancements [29, 31, 45], video generation has lagged behind. Recent works, such as VideoTetris [40] and Vico [47], have improved compositional variations and temporal consistency but still face difficulties in handling dynamic object interactions. Layout-based approaches, such as LVD [26], often lack precise spatiotemporal guidance. More recent methods leverage large language models (LLMs) [19, 24, 28] to enhance compositional control through fine-grained scene planning. Although effective, these approaches require substantial computational resources for training. In contrast, MagicComp, the proposed method, operates within a training-free framework, making it a more efficient solution.

3. Method

3.1. Overall Framework of MagicComp

As illustrated in Figure 2, MagicComp employs a dual-phase refinement strategy during the sampling process. In the conditioning stage, SAD module performs an additional encoding step, processing each subject in the prompt independently to generate semantically purified anchor embeddings. These anchors are then used to compute semantic directional vectors, which are adaptively fused into the original prompt embeddings to mitigate semantic leakage and ambiguity between subjects (see Sec. 3.2). In the denoising

stage, DLFA applies fine-grained subject-aware masked attention by combining prior LLM layout masks with model-adaptive perception masks. The prior masks provide coarse estimates of subject size and position, while the model-adaptive perception masks, derived from text-video embedding correlations, enable precise manipulation of subject shapes and details. Overall, the integration of both stages allows for training-free generation of compositional videos, eliminating semantic ambiguity while ensuring precise attribute–location binding.

3.2. Semantic Anchor Disambiguation

As revealed in [18, 44], text encoders such as T5 [37] and CLIP [36] allow tokens to interact with each other during the encoding process, which may cause semantic leakage between subjects with fine-grained attributes or similar semantics. As illustrated in Figure 3, the T5 embeddings of “brown dog” and “gray cat” exhibit remarkably high similarity, disrupting the text-video attention correlation between these two subjects and resulting in visually confused content (e.g., a cat resembling a dog).

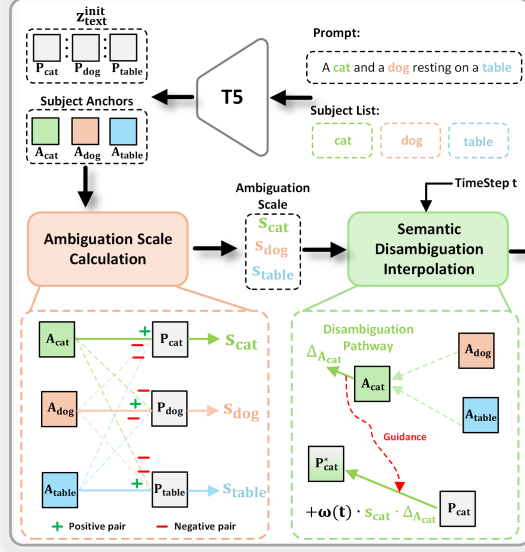
To mitigate these issues, SAD module is proposed to eliminate semantic confusion between subjects and provide a more instructive conditional text embedding. For a prompt containing M subjects, SAD module first obtains the embedding representation P and the corresponding subject token embeddings $[P_i]_{i=1}^M = [P_1, P_2, \dots, P_M]$. Following this, it independently encodes each subject in the prompt to obtain the subject anchor embeddings $[A_i]_{i=1}^M = [A_1, A_2, \dots, A_M]$. The core of SAD module lies in leveraging the pure semantic information of each subject in $[A_i]_{i=1}^M$ to appropriately eliminate semantic confusion while preserving the contextual relationships in $[P_i]_{i=1}^M$. Specifically, SAD module first calculates the confusion scale to quantify semantic confusion, then adjusts the intensity of semantic disambiguation interpolation accordingly.

Confusion Scale Calculation. For subject k , an intuitive way to assess its semantic confusion is to evaluate the extent to which it deviates from its original semantics while converging towards the semantics of other subjects. This can be quantified as the degree to which P_k moves away from A_k and closer to $[A_i]_{i=1}^M$ (where $i \neq k$) in the semantic space:

$$s_k = \frac{\sum_{i=1}^M 1_{[i \neq k]} \exp(\cos(\overline{P}_k, \overline{A}_i) / \tau)}{\sum_{i=1}^M \exp(\cos(\overline{P}_k, \overline{A}_i) / \tau)}. \quad (1)$$

where s_k denotes the confusion scale for subject k , \overline{P}_k and \overline{A}_i refers to pooled embeddings and τ indicates the temperature factor which is experimentally set to 0.2. Similarly, confusion scale for all the subjects can be represented as $[s_i]_{i=1}^M$, which are then utilized as the scaling factors for the strength of semantic disambiguation interpolation.

(a) Semantic Anchor Disambiguation



(b) Dynamic Layout Fusion Attention

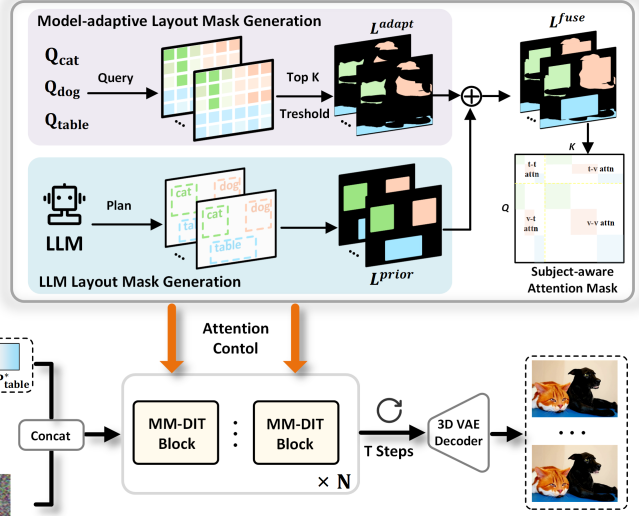


Figure 2. **Detailed architecture of MagicComp.** The dual-phase refinement strategy of MagicComp contains two core steps: (a) Semantic Anchor Disambiguation (SAD) module for inter-subject disambiguation during the conditioning stage. We only display disambiguation process of subject “cat” for simplicity, other subjects follow the similar way. (b) Dynamic Layout Fusion Attention (DLFA) module for precise attribute–location binding of each subject during the denoising stage.

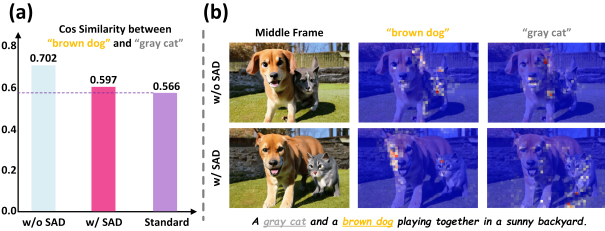


Figure 3. **Visualization of the disambiguation effect brought by SAD.** (a) Cos similarity between the pooled embeddings of “brown dog” and “gray cat” under different settings. “Standard” indicates the cos similarity is computed when each subject are independently encoded by T5. (b) Cross attention maps between the middle frame video tokens and the pooled subject tokens.

Semantic Disambiguation Interpolation. To disambiguate the semantics of subject k , we must identify the pathways in the semantic space that direct it away from the semantic of other subjects and closer to its own. Specifically, the pathway can be represented as the semantic directional vector Δ_{A_k} from other subjects to subject k using the pooled subject anchor embeddings $[\bar{A}_i]_{i=1}^M$:

$$\Delta_{A_k} = \sum_{i=1}^M (\bar{A}_k - \bar{A}_i). \quad (2)$$

The semantic directional vectors for all the subjects $[\Delta_{A_i}]_{i=1}^M$ can be obtained in a similar manner.

After obtaining $[\Delta_{A_i}]_{i=1}^M$, we can interpolate it into the

original embeddings $[P_i]_{i=1}^M$ to eliminate semantic confusion according to the confusion scales $[s_i]_{i=1}^M$. However, determining the appropriate interpolation strength should also consider the specific denoising time step. Since the early stages of denoising require clearer semantics to capture the basic layout and shape of each subject, while the later stages of denoising focus more on leveraging the context restored in $[P_i]_{i=1}^M$ to understand the interactions between different subjects. To achieve this, we additionally incorporate a time-aware strength attenuated function $\omega(t) = 1 - \frac{t}{T}$ to formulate the final interpolation process:

$$P_i^* = P_i \oplus (\omega(t) \cdot s_i \cdot \Delta_i). \quad (3)$$

where P_i^* indicates the interpolated subject embeddings, and \oplus refers to the broadcasting, respectively. Finally, $[P_i]_{i=1}^M$ is replaced by $[P_i^*]_{i=1}^M$ to obtain the semantically disambiguated condition. As shown in Figure 3, after incorporating the SAD module, the semantic similarity between “brown dog” and “gray cat” approaches a normal level, and their cross-attention maps in the subsequent denoising stage exhibit a decoupled pattern. This further demonstrates the effectiveness of the SAD module.

3.3. Dynamic Layout Fusion Attention

To conduct spatio-temporal binding between each subject and its respective textual attributes and locations, DLFA is devised to dynamically guide the subject-specific region conditioning on the corresponding subject in the text

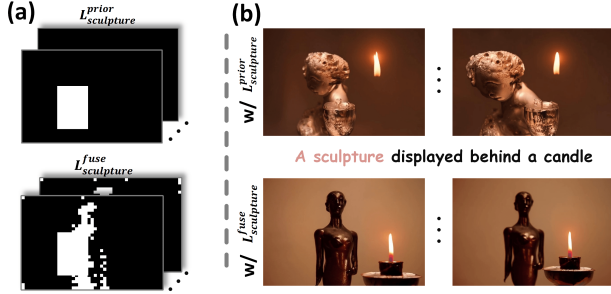


Figure 4. **Comparison of different masking strategy.** (a) Visualization of prior layout mask and model-adaptive perception layout. (b) Comparison of the generated videos.

prompt. Unlike training-based methods relying solely on prior layout masks [12, 26, 43], DLFA conducts the subject-aware masked attention via a coarse-to-fine masking strategy: first coarsely localizing subjects via prior layout mask generated by LLM, then refining their shapes and details through the introduction of model-adaptive perception layout mask.

Prior Layout Mask. Given M subjects specified in the prompt, we utilize LLM to automatically generate prior layouts $L^{prior} = \{L_1^{prior}, L_2^{prior}, \dots, L_M^{prior}\}$, where $L_i^{prior} \in \{0, 1\}^{N_{video}}$ indicates the binary layout mask for i -th subject with the number of the video tokens N_{video} . Concurrently, we extract corresponding textual token masks $T^{subject} = \{T_1^{subject}, T_2^{subject}, \dots, T_M^{subject}\}$, where $T_i^{subject} \in \{0, 1\}^{N_{text}}$ with N_{text} being the number of textual tokens.

Model-adaptive Perception Layout Mask. Unfortunately, the prior layout masks often manifest as coarse 2D bounding boxes, which is misaligned with the diverse geometric profiles of real-world subjects. To address this limitation, we introduce an additional model-adaptive perception layout that is dynamically derived from video tokens exhibiting strong cross-modal correlations with their corresponding subject tokens. Given text query for subjects $\{Q_1^{text}, Q_2^{text}, \dots, Q_M^{text}\}$ and video key K^{video} , we first obtain the attention correlation $Corr_i$ for the i -th subject:

$$Corr_i = \overline{Q_i^{text}} K^{video \top}. \quad (4)$$

where $\overline{Q_i^{text}}$ indicates the pooled embedding for the i -th subject token. Afterwards, the problem lies in how to determine an appropriate correlation threshold to define the model-perceived layout. Fortunately, the prior layouts L^{prior} already includes approximate information about object sizes, which serve as size references for deriving

subject-specific thresholds:

$$\begin{aligned} k &= \text{CountTrue}(L_i^{prior}). \\ \delta_i &= \text{Sort}_{(k)}^{\text{desc}}(Corr_i). \end{aligned} \quad (5)$$

where δ_i refers to the threshold for the i -th subject and $\text{Sort}_{(k)}^{\text{desc}}(\cdot)$ is the operator that retrieves the k -th largest value. We then threshold the attention correlation for each subject:

$$L_i^{adapt} = \mathbb{I}(Corr_i > \delta_i). \quad (6)$$

Similarly, we can obtain the model-adaptive perception layouts $L^{adapt} = \{L_1^{adapt}, L_2^{adapt}, \dots, L_M^{adapt}\}$.

Subject-aware Masked Attention. After constructing the prior layout masks L^{prior} and model-adaptive perception layout masks L^{adapt} , we combine these two types of masks for each subject individually:

$$\begin{aligned} L_i^{fuse} &= L_i^{prior} \cup L_i^{adapt}, \\ L^{fuse} &= \{L_1^{fuse}, L_2^{fuse}, \dots, L_M^{fuse}\}. \end{aligned} \quad (7)$$

The fused masks, L^{fuse} , incorporate both the subject’s position and size as determined by the LLM, along with the object’s shape dynamics and details, which are adaptively perceived by the model. As a result, we can leverage L^{fuse} to conduct subject-aware masked attention in MM-DiT [48]. Following the similar way in [40, 43], the masking strategy adheres to the following principle: For subject i , we only allow attention interactions between its corresponding video tokens within the layout L_i^{fuse} and the text tokens associated with subject i , ensuring precise subject binding and inter-frame consistency. For video tokens outside the layout regions and text tokens unrelated to the subjects, we enable unrestricted interactions with all tokens to ensure contextual coherence (see Appendix 1 for details). Furthermore, to explicitly enforce alignment between generated subjects and their predefined layouts L^{fuse} , we introduce a localized independent noise sampling strategy, which conducts initial noise sampling independently within each subject’s designated layout region.

As shown in Figure 4, DLFA captures shape dynamic of the subject, thereby enabling more flexible attribute-location binding compared to static prior layout masks.

4. Experiment

The setups are described in Section 4.1. Quantitative and qualitative comparisons are provided in Sections 4.2 and 4.3, respectively. Ablation studies are discussed in Section 4.4. Various applications are showcased in Section 4.5.

4.1. Experimental Setups

Implementation Details. We build upon the diffusers for video generation and develop MagicComp using two main-stream models: CogVideoX [48], which adopts a DiT-based

Model	T2V-CompBench						VBench	
	Consist-attr	Spatial	Motion	Action	Interaction	Numeracy	Multi-obj	Spatial-rela
<i>T2V model:</i>								
ModelScope [41]	0.5483	0.4220	0.2662	0.4880	0.7075	0.2066	0.3898	0.3409
ZeroScope [2]	0.4495	0.4073	0.2319	0.4620	0.5550	0.2378	-	-
Latte [30]	0.5325	0.4476	0.2187	0.5200	0.6625	0.2187	0.3453	0.4153
VideoCrafter2 [8]	0.6750	0.4891	0.2233	0.5800	0.7600	0.2041	0.4066	0.3586
Open-Sora 1.2 [54]	0.6600	0.5406	0.2388	0.5717	0.7400	0.2556	0.5183	0.6856
Open-Sora-Plan v1.1.0 [27]	0.7413	0.5587	0.2187	0.6780	0.7275	0.2928	0.4035	0.5311
AnimateDiff [14]	0.4883	0.3883	0.2236	0.4140	0.6550	0.0884	0.3831	0.4428
Pika [†] [35]	0.6513	0.5043	0.2221	0.5380	0.6625	0.2613	0.4308	0.6103
Gen-3 [†] [5]	0.7045	0.5533	<u>0.3111</u>	0.6280	0.7900	0.2169	0.5364	0.6509
Dream Machine [†] [4]	0.6900	0.5397	0.2713	<u>0.6400</u>	0.7725	0.2109	-	-
<i>Compositional T2V model:</i>								
LVD [26]	0.5595	0.5469	0.2699	0.4960	0.6100	0.0991	-	-
VideoTetris [40]	0.7125	0.5148	0.2204	0.5280	0.7600	0.2609	-	-
DreamRunner [43]	0.7350	0.6040	0.2608	0.5840	0.8225	-	-	-
Vico [47]	0.6980	0.5432	0.2412	0.6020	0.7800	-	<u>0.6321</u>	-
VideoRepair [24]	<u>0.7475</u>	0.6000	-	-	-	<u>0.2931</u>	-	-
CogVideoX-2B [48]	0.6775	0.4848	0.2379	0.5700	0.7250	0.2568	0.6263	<u>0.6990</u>
CogvideoX-2B + Ours	0.7665	<u>0.6012</u>	0.3192	0.6140	<u>0.8025</u>	0.3079	0.6659	0.7325

Table 1. Evaluation results on T2V-CompBench and VBench. "T2V-Comp" includes six evaluation metrics, while "VBench" introduces two new metrics: "Multi-obj" and "Spatial-rela". Best/2nd best scores are **bolded/underlined**. † indicates the commercial models.

Model	Consist-attr	Spatial	Interaction	Numeracy	Time
CogvideoX-2B	0.6775	0.4848	0.7250	0.2568	75s
w/ SAD	0.7225	0.5353	0.7575	0.2845	77s
w/ DLFA	0.7380	0.5734	0.7800	0.2964	85s
w/ DLFA & SAD	0.7665	0.6012	0.8025	0.3079	87s
VideoCrafter2	0.6750	0.4891	0.7600	0.2041	14s
w/ SAD	0.7020	0.5132	0.7625	0.2294	15s
w/ DLFA	0.7125	0.5349	0.7850	0.2463	16s
w/ DLFA & SAD	0.7203	0.5435	0.7900	0.2553	17s

Table 2. Ablation study of SAD and DLFA modules. Removing any of these modules significantly reduces model performance.

Model	Consist-attr	Spatial	Interaction	Numeracy
CogvideoX-2B	0.6775	0.4848	0.7250	0.2568
w/ 3D Region Attention	0.7248	0.5632	0.7625	0.2878
w/ DLFA	0.7380	0.5734	0.7800	0.2964
w/ Word Swap	0.6995	0.4767	0.7275	0.2463
w/ SAD	0.7225	0.5353	0.7575	0.2845

Table 3. Ablation study on incorporating other approaches on CogvideoX-2B. Replacing SAD and DLFA with other naive strategies leads to a performance drop.

architecture, and VideoCrafter2 [8], which utilizes a UNet-based design. All videos are generated on an A100 GPU.

Evaluated Models. We compare our approach against two groups of baseline models: text-to-video (T2V) models and compositional T2V models. The T2V base models include ModelScope [41], ZeroScope [2], Latte [30], VideoCrafter2 [8], Open-Sora 1.2 [54], Open-Sora-Plan

v1.1.0 [27] and AnimateDiff [14], as well as the commercially available closed-source models Pika [1], Gen-3 [5] and Dream Machine [4]. The compositional T2V models include LVD [26], VideoTetris [40], DreamRunner [43], Vico [47], and VideoRepair [24].

Benchmark and Evaluation Metrics. We employ two widely-used T2V generation benchmarks, T2V-CompBench [39] and VBench [20], for evaluation. These benchmarks comprehensively assess the alignment between text prompts and generated videos across various scenarios.

For T2V-CompBench, we select six categories to examine compositional abilities in text-to-video generation: consistent attribute binding, spatial relationships, motion binding, action binding, object interactions, and generative numeracy, with each category containing 100 prompts. For VBench, two evaluation aspects are utilized: multiple objects and spatial relationships.

4.2. Quantitative Comparisons

We conduct a comprehensive quantitative evaluation of different methods, and the results are presented in Table 1. Our method demonstrates outstanding performance across multiple evaluation metrics. Specifically, Magic-Comp achieves the highest scores in *Consist-attr*, *Motion*, *Numeracy*, *Multi-obj*, and *Spatial-rela*, outperforming all other models in these categories. Among T2V models, Open-Sora-Plan v1.1.0 [27] and Dream Machine [4] obtain the highest *Action* scores, while Gen-3 [5] performs

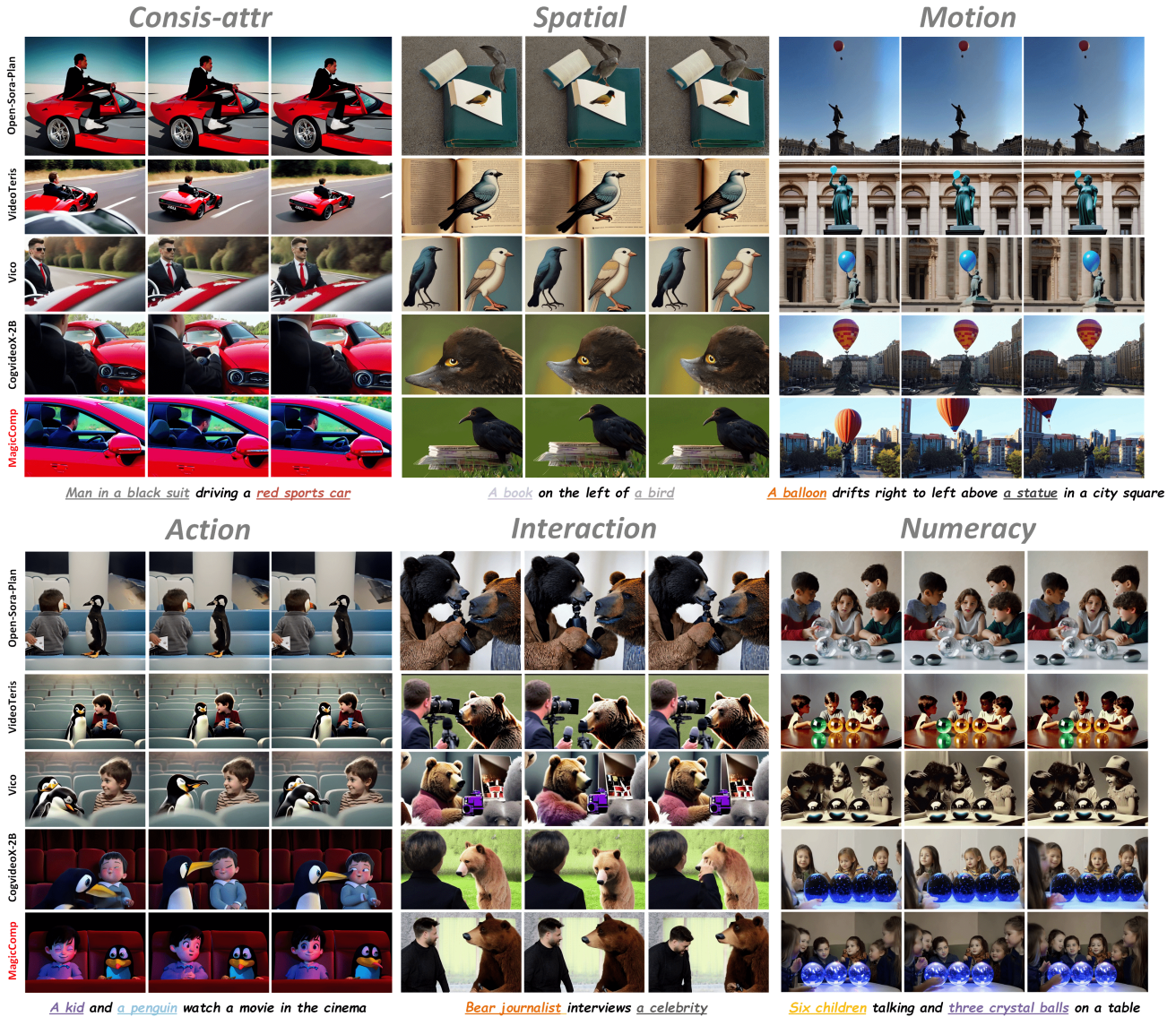


Figure 5. **Qualitative Comparison on T2V-CompBench.** Our MagicComp significantly outperforms existing approaches across various compositional generation tasks, and the methods such as Vico [47] and CogVideoX [48] struggle to capture fine-grained concepts.

well in *Motion* but still falls behind our model. For compositional T2V models, although DreamRunner [43] excels in *Spatial* and *Interaction*, and VideoRepair [28] achieves the best *Consist-attr* score, while Vico [47] demonstrates strong *Multi-obj* performance, these models require substantial computational resources to generate videos. In contrast, MagicComp is a low-cost, zero-shot approach that effectively captures fine-grained object relationships, understands numerical dependencies, and preserves consistent compositional attributes. These results verify the effectiveness of our method in compositional T2V generation.

4.3. Qualitative Comparisons

This section qualitatively compares the generation quality across consistency attributes, spatial relations, motion, action, interaction dynamics, and numerical understanding among Open-Sora-Plan [27], VideoTeris [40], Vico [47], CogVideoX-2B [48], and our proposed MagicComp. Specifically, we select representative prompts from the T2V-CompBench for analysis, as shown in Figure 5. Open-Sora-Plan, VideoTeris, Vico, and CogVideoX-2B struggle to maintain consistent object attributes and spatial relationships, resulting in inaccurate visual representations and compromised temporal coherence. For instance, in

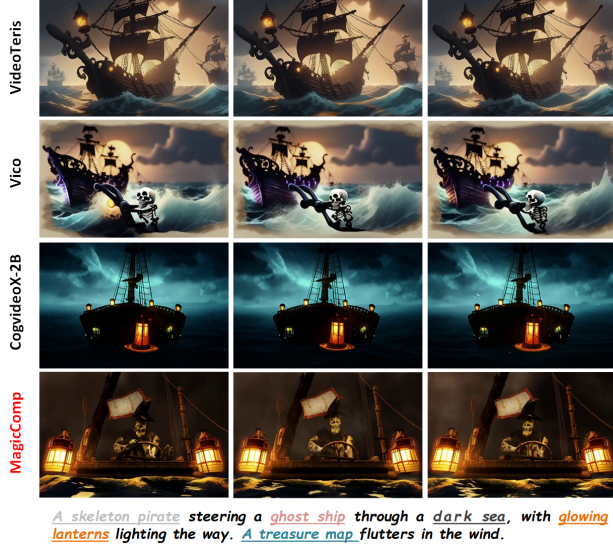


Figure 6. **Application on complex prompt-based video generation.** It is evident that among all models, only MagicComp strictly follows the prompt to generate complex scenarios.

depicting spatial relations (e.g., "A book on the left of a bird"), Vico and VideoTeris show limited spatial comprehension, whereas MagicComp demonstrates clear and accurate scene layout understanding. In action and interaction dynamics, MagicComp outperforms all comparative methods by capturing and maintaining coherent actions throughout the generated frames. Moreover, in evaluating numeracy prompts, MagicComp distinctly showcases improved numerical comprehension and precise scene composition. These qualitative findings demonstrate that MagicComp consistently surpasses existing methods, including those trained extensively, highlighting the effectiveness of our training-free framework in accurately modeling various compositional and relational concepts. For additional qualitative comparisons, please refer to the Appendix.

4.4. Ablation Study

We conduct ablation studies on SAD and DLFA modules to evaluate their effectiveness. As shown in Table 2, integrating SAD module into the baseline CogvideoX-2B model significantly improves all metrics. Specifically, *Consist-attr* increases from 0.6775 to 0.7225, *Spatial* improves from 0.4848 to 0.5353, *Interaction* rises from 0.7250 to 0.7575, and *Numeracy* advances from 0.2568 to 0.2845. These results underscore the effectiveness of SAD in resolving semantic ambiguities. Furthermore, incorporating the DLFA module yields additional enhancements, confirming its ability to adaptively enhance spatial and interactional information. Combining SAD and DLFA modules together produces the highest overall performance, which proves their collaborative effectiveness. Furthermore, we conduct simi-

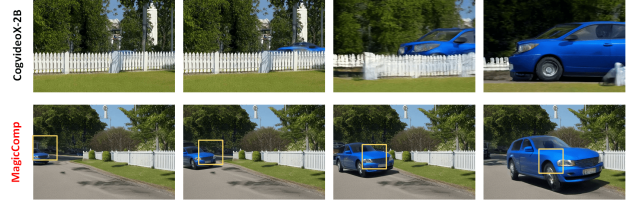


Figure 7. **Application about trajectory-controllable video generation.** By incorporating the proposed methods, CogVideoX [48] can achieve trajectory control seamlessly without additional cost.

lar experiments using the VideoCrafter2 model, where consistent performance improvements are observed after introducing SAD and DLFA. This further validates the generalizability of our proposed modules across diverse model architectures. More importantly, adding SAD and DLFA to CogVideoX and VideoCrafter2 increases inference time by only 16% and 21.4%, respectively, demonstrating the efficiency of the proposed methods.

Moreover, we conduct another ablation study on CogVideoX-2B (see Table 3) to assess the advantage of the proposed methods over other naive strategies. Comparing with 3D Region Attention [43], we find that DLFA outperforms 3D Region Attention across all evaluation metrics. Moreover, directly replacing subject embeddings with semantic anchors (i.e., Word Swap) causes a significant performance drop, proving the effectiveness of SAD in dynamically integrating semantic directional vectors into the original embeddings. Collectively, these results confirm the effectiveness of the proposed SAD and DLFA modules.

4.5. Applications

We further demonstrate the practical applicability of MagicComp in more complex and challenging scenarios. Figure 6 showcases its effectiveness in complex prompt-driven video generation, successfully interpreting a sophisticated textual description involving multiple intricate elements, such as a skeleton pirate, a ghost ship, a dark sea, glowing lanterns, and a treasure map. Additionally, Figure 7 highlights MagicComp’s capability in trajectory-controllable video generation, effectively guiding object movements along specified paths while significantly outperforming existing methods. These results further highlight MagicComp’s potential for a broader range of video generation tasks.

5. Conclusion

In this paper, we introduce **MagicComp**, a novel training-free approach designed to address critical limitations in compositional text-to-video (T2V) generation, particularly in attribute binding, spatial relationship reasoning, and multi-object consistency. Our Semantic Anchor Disambiguation (SAD) and Dynamic Layout Fusion Attention (DLFA) modules effectively refine semantic interpretation

and enhance localized attention. Extensive experiments demonstrate that MagicComp consistently achieves superior performance over state-of-the-art methods, validating its versatility and generalization capabilities across different benchmarks, such as T2V-CompBench and VBench. Given its model-agnostic and flexible nature, MagicComp offers a robust framework applicable to diverse T2V architectures, thus providing promising potential for future research directions, including complex prompt-driven and trajectory-controllable video generation tasks.

References

- [1] Pika. <https://www.pika.art/>, 2023. 2, 6
- [2] Zeroscope. https://huggingface.co/cerspense/zeroscope_v2_576w, 2023. 3, 6
- [3] Dreamina. <https://dreamina.capcut.com/ai-tool/platform>, 2024. 2
- [4] Luma ai. <https://lumalabs.ai/dream-machine>, 2024. 6
- [5] Gen-3. <https://runwayml.com/blog/introducing-gen-3-alpha/>, 2024. 2, 6
- [6] Andreas Blattmann, Robin Rombach, Huan Ling, Tim Dockhorn, Seung Wook Kim, Sanja Fidler, and Karsten Kreis. Align your latents: High-resolution video synthesis with latent diffusion models. In *Proceedings of the IEEE/CVF Conference on Computer Vision and Pattern Recognition*, pages 22563–22575, 2023. 3
- [7] Minghong Cai, Xiaodong Cun, Xiaoyu Li, Wenze Liu, Zhaoyang Zhang, Yong Zhang, Ying Shan, and Xiangyu Yue. Ditctrl: Exploring attention control in multi-modal diffusion transformer for tuning-free multi-prompt longer video generation. *arXiv preprint arXiv:2412.18597*, 2024. 3
- [8] Haoxin Chen, Yong Zhang, Xiaodong Cun, Menghan Xia, Xintao Wang, Chao Weng, and Ying Shan. Videocrafter2: Overcoming data limitations for high-quality video diffusion models. *arXiv preprint arXiv:2401.09047*, 2024. 2, 3, 6
- [9] Liuhan Chen, Zongjian Li, Bin Lin, Bin Zhu, Qian Wang, Shenghai Yuan, Xing Zhou, Xinhua Cheng, and Li Yuan. Od-vae: An omni-dimensional video compressor for improving latent video diffusion model. *arXiv preprint arXiv:2409.01199*, 2024. 3
- [10] Patrick Esser, Sumith Kulal, Andreas Blattmann, Rahim Entezari, Jonas Müller, Harry Saini, Yam Levi, Dominik Lorenz, Axel Sauer, Frederic Boesel, Dustin Podell, Tim Dockhorn, Zion English, Kyle Lacey, Alex Goodwin, Yan-nik Marek, and Robin Rombach. Scaling rectified flow transformers for high-resolution image synthesis, 2024. 2
- [11] Weixi Feng, Chao Liu, Sifei Liu, William Yang Wang, Arash Vahdat, and Weili Nie. Blobgen-vid: Compositional text-to-video generation with blob video representations. *arXiv preprint arXiv:2501.07647*, 2025. 3
- [12] Weixi Feng, Chao Liu, Sifei Liu, William Yang Wang, Arash Vahdat, and Weili Nie. Blobgen-vid: compositional text-to-video generation with blob video representations. *arXiv preprint arXiv:2501.07647*, 2025. 2, 5
- [13] Team GLM, Aohan Zeng, Bin Xu, Bowen Wang, Chenhui Zhang, Da Yin, Dan Zhang, Diego Rojas, Guanyu Feng, Hanlin Zhao, et al. Chatglm: A family of large language models from glm-130b to glm-4 all tools. *arXiv preprint arXiv:2406.12793*, 2024. 2
- [14] Yuwei Guo, Ceyuan Yang, Anyi Rao, Zhengyang Liang, Yaohui Wang, Yu Qiao, Maneesh Agrawala, Dahua Lin, and Bo Dai. Animatediff: Animate your personalized text-to-image diffusion models without specific tuning. In *The Twelfth International Conference on Learning Representations*, 2024. 3, 6
- [15] Yoav HaCohen, Nisan Chiprut, Benny Brazowski, Daniel Shalem, Dudu Moshe, Eitan Richardson, Eran Levin, Guy Shiran, Nir Zabari, Ori Gordon, et al. Ltx-video: Realtime video latent diffusion. *arXiv preprint arXiv:2501.00103*, 2024. 2, 3
- [16] Wenyi Hong, Ming Ding, Wendi Zheng, Xinghan Liu, and Jie Tang. Cogvideo: Large-scale pretraining for text-to-video generation via transformers. *arXiv preprint arXiv:2205.15868*, 2022. 2
- [17] Edward J Hu, Yelong Shen, Phillip Wallis, Zeyuan Allen-Zhu, Yuanzhi Li, Shean Wang, Lu Wang, Weizhu Chen, et al. Lora: Low-rank adaptation of large language models. *ICLR*, 1(2):3, 2022. 2
- [18] Taihang Hu, Linxuan Li, Joost van de Weijer, Hongcheng Gao, Fahad Shahbaz Khan, Jian Yang, Ming-Ming Cheng, Kai Wang, and Yaxing Wang. Token merging for training-free semantic binding in text-to-image synthesis. *Advances in Neural Information Processing Systems*, 37:137646–137672, 2025. 3
- [19] Kaiyi Huang, Yukun Huang, Xuefei Ning, Zinan Lin, Yu Wang, and Xihui Liu. Genmac: compositional text-to-video generation with multi-agent collaboration. *arXiv preprint arXiv:2412.04440*, 2024. 2, 3
- [20] Ziqi Huang, Yinan He, Jiashuo Yu, Fan Zhang, Chenyang Si, Yuming Jiang, Yuanhan Zhang, Tianxing Wu, Qingyang Jin, Nattapol Chanpaisit, et al. Vbench: Comprehensive benchmark suite for video generative models. In *Proceedings of the IEEE/CVF Conference on Computer Vision and Pattern Recognition*, pages 21807–21818, 2024. 2, 6
- [21] Levon Khachatryan, Andranik Movsisyan, Vahram Tadevosyan, Roberto Henschel, Zhangyang Wang, Shant Navasardyan, and Humphrey Shi. Text2video-zero: Text-to-image diffusion models are zero-shot video generators. In *ICCV*, 2023. 3
- [22] Weijie Kong, Qi Tian, Zijian Zhang, Rox Min, Zuozhuo Dai, Jin Zhou, Jiangfeng Xiong, Xin Li, Bo Wu, Jianwei Zhang, et al. Hunyuanvideo: A systematic framework for large video generative models. *arXiv preprint arXiv:2412.03603*, 2024. 2
- [23] Weijie Kong, Qi Tian, Zijian Zhang, Rox Min, Zuozhuo Dai, Jin Zhou, Jiangfeng Xiong, Xin Li, Bo Wu, Jianwei Zhang, et al. Hunyuanvideo: A systematic framework for large video generative models. *arXiv preprint arXiv:2412.03603*, 2024. 3
- [24] Daeun Lee, Jaehong Yoon, Jaemin Cho, and Mohit Bansal. Videorepair: improving text-to-video generation via mis-

- alignment evaluation and localized refinement. *arXiv preprint arXiv:2411.15115*, 2024. 2, 3, 6
- [25] Zongjian Li, Bin Lin, Yang Ye, Liuhan Chen, Xinhua Cheng, Shenghai Yuan, and Li Yuan. Wf-vae: Enhancing video vae by wavelet-driven energy flow for latent video diffusion model. *arXiv preprint arXiv:2411.17459*, 2024. 2, 3
- [26] Long Lian, Baifeng Shi, Adam Yala, Trevor Darrell, and Boyi Li. Llm-grounded video diffusion models. In *ICLR*, 2024. 2, 3, 5, 6
- [27] Bin Lin, Yunyang Ge, Xinhua Cheng, Zongjian Li, Bin Zhu, Shaodong Wang, Xianyi He, Yang Ye, Shenghai Yuan, Liuhan Chen, et al. Open-sora plan: Open-source large video generation model. *arXiv preprint arXiv:2412.00131*, 2024. 2, 3, 6, 7
- [28] Han Lin, Abhay Zala, Jaemin Cho, and Mohit Bansal. Videodirectorgpt: Consistent multi-scene video generation via llm-guided planning. *arXiv preprint arXiv:2309.15091*, 2023. 3, 7
- [29] Nan Liu, Shuang Li, Yilun Du, Antonio Torralba, and Joshua B Tenenbaum. Compositional visual generation with composable diffusion models. In *European Conference on Computer Vision*, pages 423–439. Springer, 2022. 3
- [30] Xin Ma, Yaohui Wang, Gengyun Jia, Xinyuan Chen, Ziwei Liu, Yuan-Fang Li, Cunjian Chen, and Yu Qiao. Latte: Latent diffusion transformer for video generation. *arXiv preprint arXiv:2401.03048*, 2024. 6
- [31] Weili Nie, Sifei Liu, Morteza Mardani, Chao Liu, Benjamin Eckart, and Arash Vahdat. Compositional text-to-image generation with dense blob representations. *arXiv preprint arXiv:2405.08246*, 2024. 3
- [32] OpenAI. Video generation models as world simulators. <https://openai.com/index/video-generation-models-as-world-simulators/>, 2023. Accessed: 2024-2. 2, 3
- [33] OpenAI. Hello gpt-4o, 2024. 2
- [34] OpenAI. GPT-4 technical report, 2024. 2
- [35] Pika. Pika art 2.0’s scene ingredients: Redefining personalized video creation, 2024. Accessed: 2025-02-26. 6
- [36] Alec Radford, Jong Wook Kim, Chris Hallacy, Aditya Ramesh, Gabriel Goh, Sandhini Agarwal, Girish Sastry, Amanda Askell, Pamela Mishkin, Jack Clark, et al. Learning transferable visual models from natural language supervision. In *International conference on machine learning*, pages 8748–8763. PMLR, 2021. 3, 1
- [37] Colin Raffel, Noam Shazeer, Adam Roberts, Katherine Lee, Sharan Narang, Michael Matena, Yanqi Zhou, Wei Li, and Peter J Liu. Exploring the limits of transfer learning with a unified text-to-text transformer. *Journal of machine learning research*, 21(140):1–67, 2020. 3
- [38] Olaf Ronneberger, Philipp Fischer, and Thomas Brox. U-net: Convolutional networks for biomedical image segmentation. In *Medical Image Computing and Computer-Assisted Intervention—MICCAI 2015: 18th International Conference, Munich, Germany, October 5–9, 2015, Proceedings, Part III 18*, pages 234–241. Springer, 2015. 3
- [39] Kaiyue Sun, Kaiyi Huang, Xian Liu, Yue Wu, Zihan Xu, Zhenguo Li, and Xihui Liu. T2v-compbench: A comprehensive benchmark for compositional text-to-video generation. *arXiv preprint arXiv:2407.14505*, 2024. 2, 6
- [40] Ye Tian, Ling Yang, Haotian Yang, Yuan Gao, Yufan Deng, Jingmin Chen, Xintao Wang, Zhaochen Yu, Xin Tao, Pengfei Wan, Di Zhang, and Bin Cui. Videotetris: towards compositional text-to-video generation. In *NeurIPS*, 2024. 2, 3, 5, 6, 7
- [41] Jiuniu Wang, Hangjie Yuan, Dayou Chen, Yingya Zhang, Xiang Wang, and Shiwei Zhang. Modelscope text-to-video technical report. *arXiv preprint arXiv:2308.06571*, 2023. 3, 6
- [42] Yaohui Wang, Xinyuan Chen, Xin Ma, Shangchen Zhou, Ziqi Huang, Yi Wang, Ceyuan Yang, Yanan He, Jiashuo Yu, Peiqing Yang, et al. Lavie: High-quality video generation with cascaded latent diffusion models. *International Journal of Computer Vision*, pages 1–20, 2024. 2
- [43] Zun Wang, Jialu Li, Han Lin, Jaehong Yoon, and Mohit Bansal. Dreamrunner: Fine-grained storytelling video generation with retrieval-augmented motion adaptation. *arXiv preprint arXiv:2411.16657*, 2024. 2, 5, 6, 7, 8
- [44] Tianyi Wei, Dongdong Chen, Yifan Zhou, and Xingang Pan. Enhancing mmdit-based text-to-image models for similar subject generation. *arXiv preprint arXiv:2411.18301*, 2024. 3
- [45] Song Wen, Guian Fang, Renrui Zhang, Peng Gao, Hao Dong, and Dimitris Metaxas. Improving compositional text-to-image generation with large vision-language models. *arXiv preprint arXiv:2310.06311*, 2023. 3
- [46] Jingyun Xue, Hongfa Wang, Qi Tian, Yue Ma, Andong Wang, Zhiyuan Zhao, Shaobo Min, Wenzhe Zhao, Kaihao Zhang, Heung-Yeung Shum, et al. Follow-your-pose v2: Multiple-condition guided character image animation for stable pose control. *arXiv preprint arXiv:2406.03035*, 2024. 3
- [47] Xingyi Yang and Xinchao Wang. Compositional video generation as flow equalization. *arXiv preprint arXiv:2407.06182*, 2024. 2, 3, 6, 7
- [48] Zhuoyi Yang, Jiayan Teng, Wendi Zheng, Ming Ding, Shiyu Huang, Jiazheng Xu, Yuanming Yang, Wenyi Hong, Xiaohan Zhang, Guanyu Feng, et al. Cogvideox: Text-to-video diffusion models with an expert transformer. *arXiv preprint arXiv:2408.06072*, 2024. 2, 3, 5, 6, 7, 8
- [49] Jiahui Yu, Yuanzhong Xu, Jing Yu Koh, Thang Luong, Gunjan Baid, Zirui Wang, Vijay Vasudevan, Alexander Ku, Yinfei Yang, Burcu Karagol Ayan, et al. Scaling autoregressive models for content-rich text-to-image generation. *arXiv preprint arXiv:2206.10789*, 2(3):5, 2022. 2
- [50] Shenghai Yuan, Jinfa Huang, Xianyi He, Yunyuan Ge, Yujun Shi, Liuhan Chen, Jiebo Luo, and Li Yuan. Identity-preserving text-to-video generation by frequency decomposition. *arXiv preprint arXiv:2411.17440*, 2024. 2, 3
- [51] Shenghai Yuan, Jinfa Huang, Yujun Shi, Yongqi Xu, Ruijie Zhu, Bin Lin, Xinhua Cheng, Li Yuan, and Jiebo Luo. Magictime: Time-lapse video generation models as metamorphic simulators. *arXiv preprint arXiv:2404.05014*, 2024. 2, 3
- [52] Shenghai Yuan, Jinfa Huang, Yongqi Xu, Yaoyang Liu, Shaofeng Zhang, Yujun Shi, Rui-Jie Zhu, Xinhua Cheng,

Jiebo Luo, and Li Yuan. Chronomagic-bench: A benchmark for metamorphic evaluation of text-to-time-lapse video generation. *Advances in Neural Information Processing Systems*, 37:21236–21270, 2025. [2](#), [3](#)

- [53] Zhenghao Zhang, Junchao Liao, Menghao Li, Zuozhuo Dai, Bingxue Qiu, Siyu Zhu, Long Qin, and Weizhi Wang. Tora: Trajectory-oriented diffusion transformer for video generation. *arXiv preprint arXiv:2407.21705*, 2024. [3](#)
- [54] Zangwei Zheng, Xiangyu Peng, Tianji Yang, Chenhui Shen, Shenggui Li, Hongxin Liu, Yukun Zhou, Tianyi Li, and Yang You. Open-sora: Democratizing efficient video production for all. *arXiv preprint arXiv:2412.20404*, 2024. [6](#)

MagicComp: Training-free Dual-Phase Refinement for Compositional Video Generation

Supplementary Material

1. Subject-aware Masked Attention in DLFA	1
2. Adapt MagicComp on VideoCrafter2	1
3. More Implementation Details	1
4. Enhanced input prompt via LLM	2
5. More Qualitative Results Demonstration	2
6. Limitation	2

1. Subject-aware Masked Attention in DLFA

We categorize the attention masks of subject-aware masked attention into two types: (1) The subject attention mask $Mask^{subject}$, which facilitates spatio-temporal binding of each subject. (2) The context attention mask $Mask^{context}$, which enables the context of text tokens and background video tokens to interact freely with all tokens.

Specifically, $Mask^{subject}$ is divided into four sub-masks based on video-text token interactions:

$$Mask^{subject} = \begin{bmatrix} Mask_{v-v}^{subject} & Mask_{v-t}^{subject} \\ Mask_{t-v}^{subject} & Mask_{t-t}^{subject} \end{bmatrix} \quad (8)$$

where $v-v$, $v-t$, $t-v$ and $t-t$ denote video-to-video, video-to-text, text-to-video, and text-to-text attentions, respectively.

For $Mask_{v-v}^{subject}$, we ensure that the visual self-attention of a subject is only applied to the corresponding tokens within its layout:

$$Mask_{v-v}^{subject} = \sum_{i=1}^M (L_i^{fuse} \otimes L_i^{fuse}). \quad (9)$$

where \otimes indicates the tensor outer product operations. Similarly, for the text self-attention $Mask_{t-t}^{subject}$, we only allow interactions between the internal tokens of a subject:

$$Mask_{t-t}^{subject} = \sum_{i=1}^M (T_i^{subject} \otimes T_i^{subject}). \quad (10)$$

Subsequently, for the cross-attention operation between video and text $Mask_{v-t}^{subject}$, we only allow interactions between the video tokens in the layout region of a subject and the text tokens belonging to the same subject:

$$Mask_{v-t}^{subject} = \sum_{i=1}^M (L_i^{fuse} \otimes T_i^{subject}). \quad (11)$$

And the cross-attention between text and video $Mask_{t-v}^{subject}$ can be obtained in a similar way:

$$Mask_{t-v}^{subject} = \sum_{i=1}^M (T_i^{subject} \otimes L_i^{fuse}). \quad (12)$$

After establishing the subject attention mask $Mask^{subject}$, we construct the context attention mask $Mask^{context}$, which allows video tokens outside the layout regions and text tokens not belonging to the subjects to interact freely with all tokens, thereby preserving global contextual coherence.

Finally, we can achieve subject-aware masked attention by injecting $Mask^{subject}$ and $Mask^{context}$ into the standard self-attention mechanism:

$$Mask^{fuse} = Mask^{subject} + Mask^{context} \\ \text{Subject-Attn} = \text{Softmax} \left(\frac{QK^T}{\sqrt{d}} \odot Mask^{fuse} \right) V. \quad (13)$$

2. Adapt MagicComp on VideoCrafter2

MagicComp can be seamlessly integrated into U-Net-based models, such as VideoCrafter2, with minimal adaptation effort. Specifically, SAD module can be directly added to the conditioning stage of VideoCrafter2, reducing semantic confusion in CLIP text embeddings [36]. For DLFA module, we utilize cross-attention to generate model-adaptive perception layout masks. After obtaining the fused layout masks, we design the attention mechanism to ensure that, within each frame, video tokens inside a subject layout region attend only to other video tokens in the same region via self-attention and interact exclusively with their corresponding subject text tokens through cross-attention. Video tokens outside the layout regions adhere to the original rules of VideoCrafter2.

3. More Implementation Details

The hyperparameters of both SAD and DLFA modules remain consistent across different model architectures. For SAD module, we cache the anchor embeddings of each subject during the conditioning stage, and only perform interpolation operations in the subsequent denoising steps, which incurs negligible additional inference overhead. For DLFA module, masked attention modulation is applied during the first 10% of the denoising process to guide the generation of global attributes (e.g., subject shapes and locations) in the early stages. For other details, please refer to Table 1.

Hyperparameters	CogVideoX	VideoCrafter2
Sampler	DPM-Solver	DPM-Solver
Denoising step	50	50
Guidance scale	12	6
Resolution	512×320	720×480
Number of frames	16	49

Table 1. **More implementation details.**

4. Enhanced input prompt via LLM

We utilize ChatGLM-4 [13] to generate coarse prior layouts for each textual prompt and extract the specified subjects. For detailed generation prompts and the corresponding data format, please refer to Figure 1.

5. More Qualitative Results Demonstration

We provide additional qualitative demonstrations highlighting the superior performance of our MagicComp across multiple critical attributes, including attribute consistency (Figures 2 and 3), motion binding and action (Figure 4 and 5), and numeracy (Figure 6), as well as specific comparisons with VideoCrafter2 in Figure 7. MagicComp consistently generates visually coherent and contextually accurate videos, clearly outperforming comparative methods on the T2V-Compbench dataset.

6. Limitation

While MagicComp significantly enhances attribute binding, spatial reasoning, and multi-object consistency in compositional video generation, its performance remains constrained by the inherent limitations of the underlying T2V architectures. Specifically, the framework may struggle with highly complex or semantically ambiguous prompts—particularly those requiring precise trajectory specifications or frame-level temporal control. Furthermore, despite being model-agnostic by design, MagicComp’s effectiveness is contingent on the pretrained backbone model’s semantic grounding and representation capabilities. Future research could further refine these aspects by exploring more sophisticated disambiguation techniques and enhanced temporal modeling strategies.

Imagine you are an annotator marking key subjects in video captions, and your annotations will guide a video generation robot to accurately generate multiple instances. The user will now provide the video caption, and would like you to recognize the critical subjects within this prompt. The required video resolution is 720x480 with 49 frames. Moreover, please plan the bounding boxes for each of the 13 key frames ONLY, which should be evenly distributed throughout the video, for these subjects. The specific requirements are as follows:

1. If the subject is a stationary object, the bounding box should remain stationary.
2. The bounding box must be normalized, with its width and height values ranging from 0 to 1, and its format specified as: [left, bottom, right, top].
3. Bounding box movement should be consistent with the motion described in the prompt.
4. The characteristic attributes of the subject (e.g., color) must be bound to the subject.
5. When encountering multiple objects, treat them as a whole. For example, for "two dogs," you should consider "two dogs" as a whole and apply one bounding box for them accordingly.

Please return the corresponding YAML file for me. Extra words will be ignored. A good example is as follows, and you should strictly follow the format of the example answer.

```

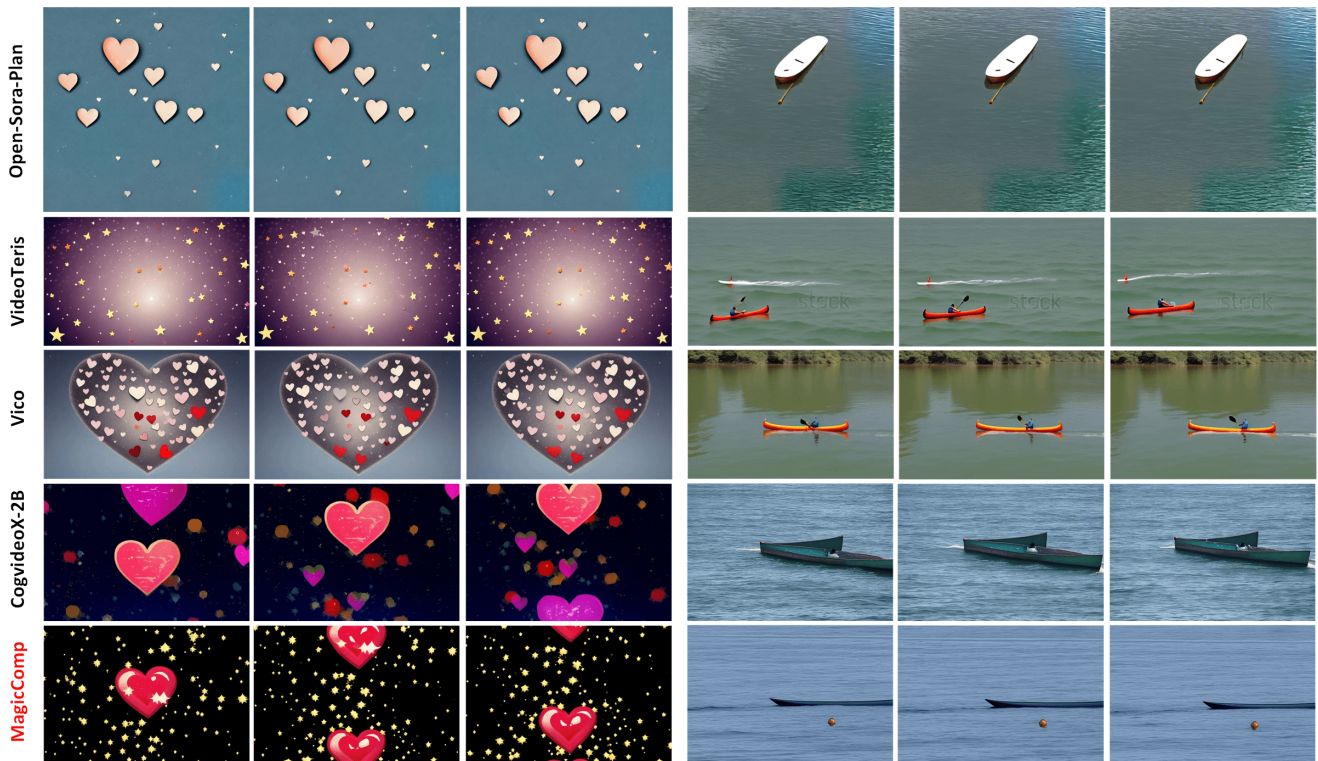
...
[INPUT]:
Annotate the key subjects in the user provided prompt and plan their motion paths using bounding boxes: "A dog runs in the park, surrounded by green grass and trees, while a man walks from the left towards the dog, with the park path ahead of him."

[OUTPUT]:
args:
protagonist:
- "A dog"
- "a man"
video_caption: "A dog runs in the park, surrounded by green grass and trees, while a man walks from the left towards the dog, with the park's path ahead of him."
frames:
- {"A dog": [0.35, 0.4, 0.55, 0.6], "a man": [0.05, 0.2, 0.15, 0.7]}
- {"A dog": [0.36, 0.4, 0.56, 0.6], "a man": [0.07, 0.2, 0.17, 0.7]}
- {"A dog": [0.37, 0.41, 0.57, 0.61], "a man": [0.10, 0.2, 0.20, 0.7]}
- {"A dog": [0.38, 0.42, 0.58, 0.62], "a man": [0.13, 0.2, 0.23, 0.7]}
- {"A dog": [0.39, 0.41, 0.59, 0.61], "a man": [0.16, 0.2, 0.26, 0.7]}
- {"A dog": [0.40, 0.40, 0.60, 0.60], "a man": [0.20, 0.2, 0.30, 0.7]}
- {"A dog": [0.41, 0.41, 0.61, 0.61], "a man": [0.24, 0.2, 0.34, 0.7]}
- {"A dog": [0.42, 0.42, 0.62, 0.62], "a man": [0.29, 0.2, 0.39, 0.7]}
- {"A dog": [0.43, 0.41, 0.63, 0.61], "a man": [0.34, 0.2, 0.44, 0.7]}
- {"A dog": [0.44, 0.40, 0.64, 0.60], "a man": [0.39, 0.2, 0.49, 0.7]}
- {"A dog": [0.45, 0.41, 0.65, 0.61], "a man": [0.44, 0.2, 0.54, 0.7]}
- {"A dog": [0.46, 0.42, 0.66, 0.62], "a man": [0.49, 0.2, 0.59, 0.7]}
- {"A dog": [0.47, 0.41, 0.67, 0.61], "a man": [0.54, 0.2, 0.64, 0.7]}
...

```

I will provide you with the video captions. You just need return the yaml file content and DO NOT return other irrelevant content. Now, let's begin generating video prompts for the subjects and plan their motion paths with bounding boxes!

Figure 1. Instruction prompt for prior layout generation.



Big hearts and small stars floating upwards

Oblong canoe gliding past a circular buoy

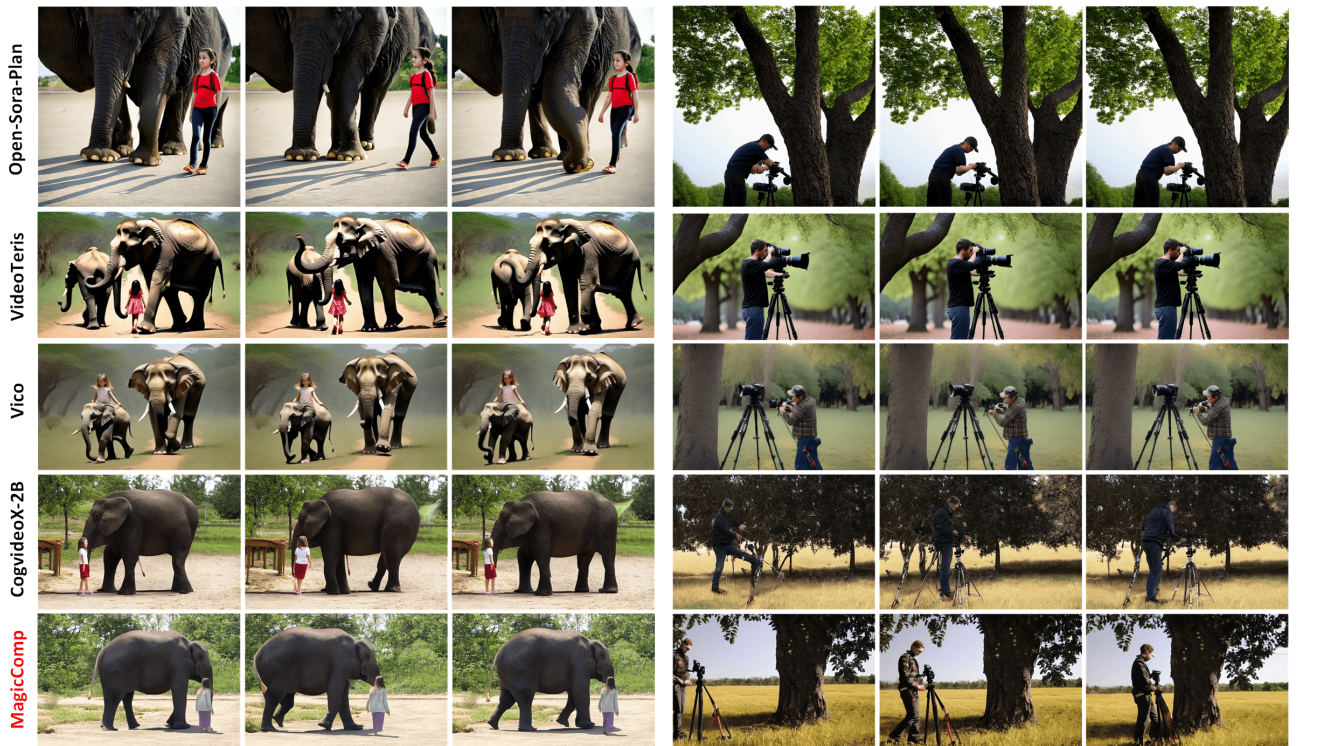
Figure 2. Qualitative results on Consist-attr.



Star-shaped cookie resting on a round coaster

Green tractor plowing near a white farmhouse

Figure 3. Qualitative results on Consist-attr.



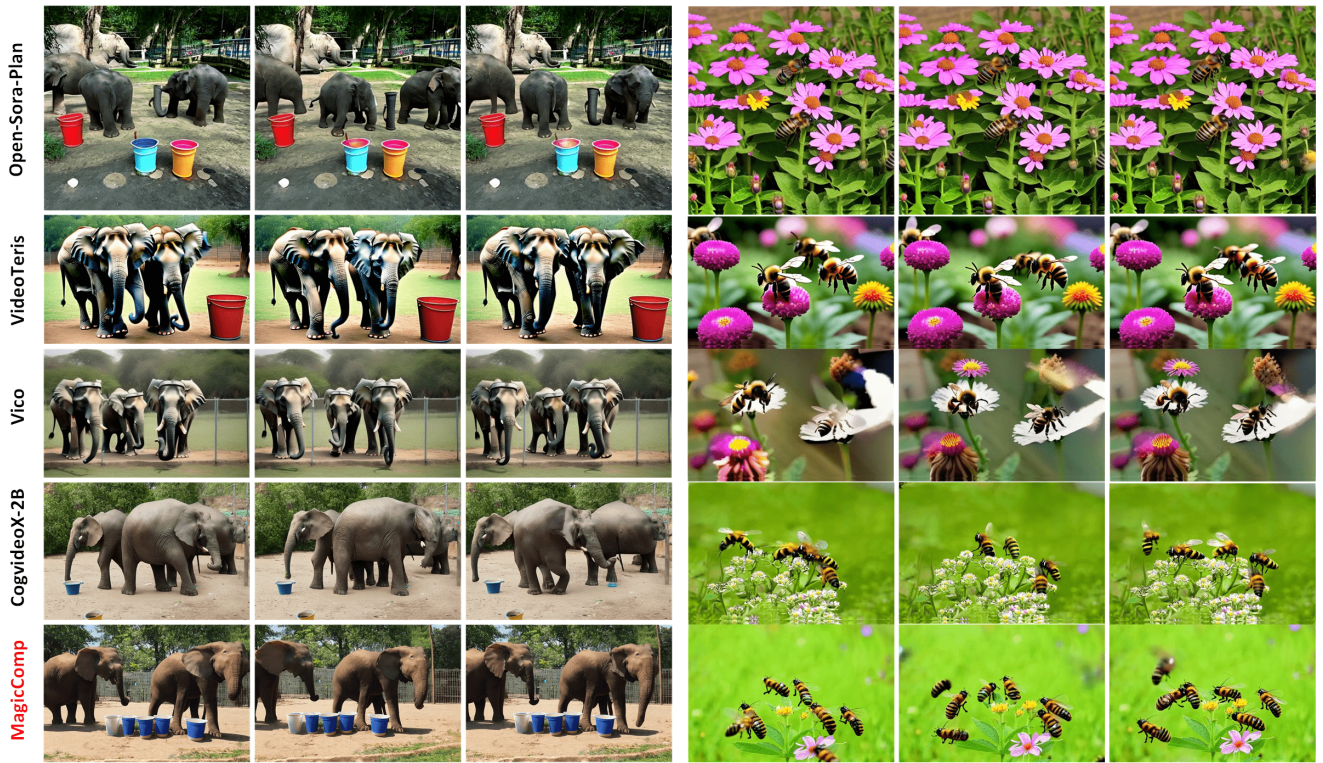
A girl walking on the right of an elephant

A photographer setting up a tripod on the left of a tree

Figure 4. Qualitative results on Motion.



Figure 5. Qualitative results on Action & Motion.



two elephants and five buckets in a zoo

seven bees buzz around a blooming flower bed

Figure 6. Qualitative results on Numeracy.

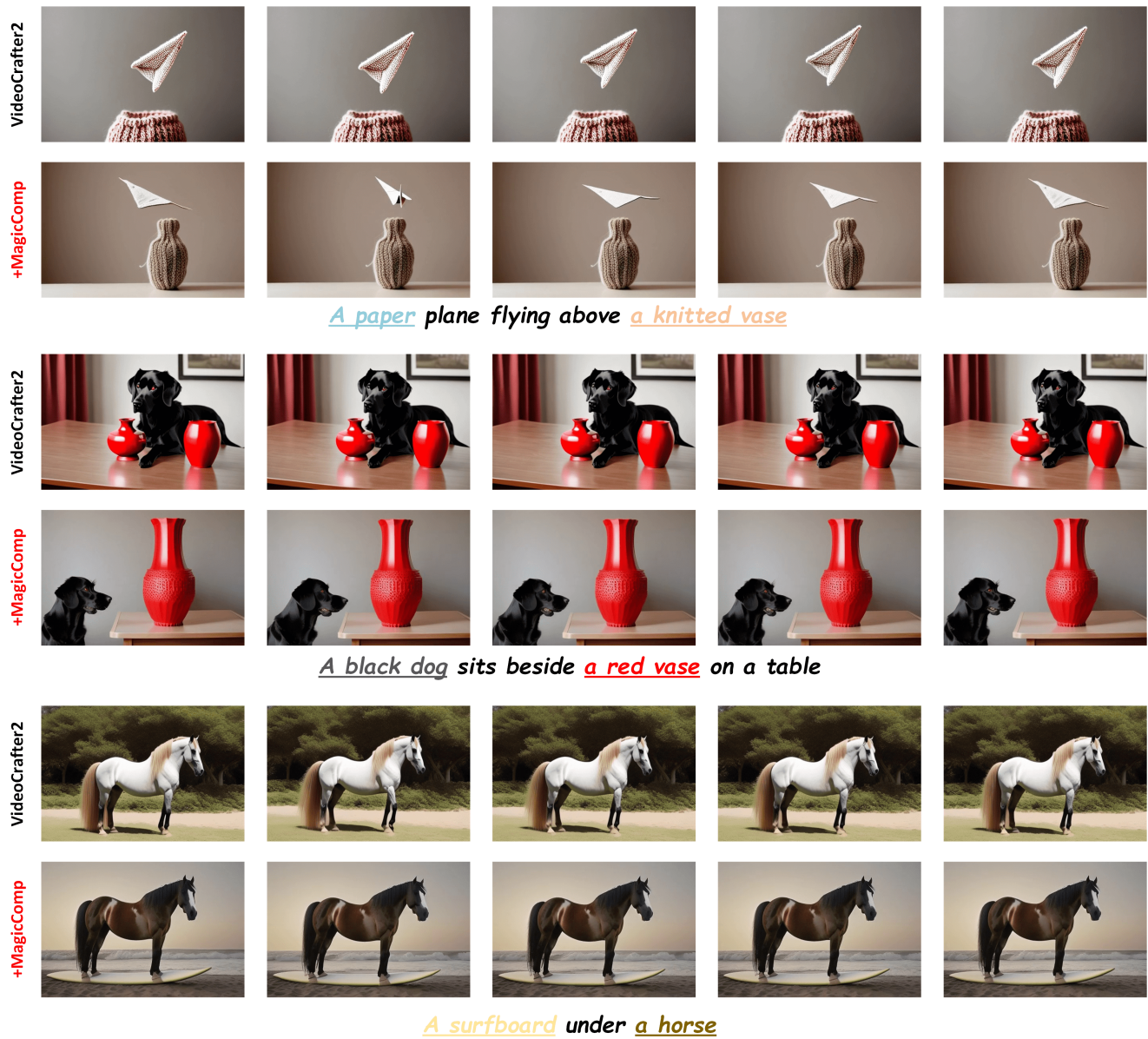


Figure 7. Qualitative results on VideoCrafter2.